JOURNAL OF COMPUTATIONAL PHYSICS 91, 478–485 (1990)

Note

Numerical Simulation of the Current–Voltage Characteristics of MIS Tunnel Devices

1. INTRODUCTION

Several studies of semiconductor devices numerical modeling have been published. In these papers the basic equations describing the working of the devices have been solved using various numerical techniques [1], e.g., finite differences, finite boxes, and finite elements which allow the discretization of the involved basic partial differential equations. Furthermore, different iterative methodes, e.g., Newton–Raphson method and Gummel's iterative algorithm, have been developed in order to solve the nonlinear algebraic system obtained from the discretized basic equations.

In this paper, we have developed a computation method for the numerical simulation of tunnel metal insulator semiconductor (MIS) structures, based on Runge–Kutta integration [2, 3] as well as on prediction-correction methods [3]. A number of theoretical or experimental studies and several models of the working of MIS structures have already been proposed in which the numerical solution is obtained by solving a set of nonlinear differential equations [4–8]. However, using some simplifications and approximations, the above equations are transformed into a set of nonlinear algebraic equations needing less CPU time [9–13]. We also point out that the rigorous solution we propose is necessary when the substrate thickness is less than the maximum width of the depletion layer; this situation is familiar for VLSI electronics.

2. BASIC EQUATION

The basic equations governing the transport of carriers in a metal-insulator-semiconductor tunnel structure in the steady-state regime are:

(a) Poisson equation [14, p. 88]; (b) current-field equations [14, p. 66]; (c) continuity equations [14, p. 66] using SHR recombination model [14, p. 46]. The above equations are completed by the appropriate boundary conditions (Section 3 and Ref. [12]). It is worth noticing here that the condition of global neutrality gives for the charges,

$$Q_{ss} + Q_f + Q_{sc} + Q_{mf} + Q_{mb} = 0. \tag{I}$$

0021-9991/90 $3.00

We introduce the charge Q_{mb} on the back contact because the electric field at $x = L$ is not equal to zero when the substrate thickness is less than the maximum width of the depletion layer.

An expression for Q_{ss} is given in [4, 12] while according to the law of Gauss we obtain:

$$Q_{mf} = C_{ox} V_{ox} = \frac{\varepsilon_0 \varepsilon_{ox}}{\delta} V_{ox} \tag{II}$$

$$Q_{mb} = \varepsilon_0 \varepsilon_s E(L) \tag{II}$$

$$Q_{sc} = -\varepsilon_0 \varepsilon_s (E(0) - E(L)). \tag{III}$$

3. Algorithm

Basic (a), (b), (c) transport equations and their boundary conditions (Section 2 and [9]) can be transformed in an equation system where Ψ, n, p, $\Psi' = d\Psi/dx = n' = dn/dx$ an $p' = dp/dx$ are regarded as six unknown functions,

$$\frac{d\Psi}{dx} = \Psi' \tag{1}$$

$$\frac{d\Psi'}{dx} = -\frac{q}{\varepsilon_0 \varepsilon_s} (p - n + N_D) \tag{2}$$

$$\frac{dn}{dx} = n' \tag{3}$$

$$\frac{dn'}{dx} = \frac{q}{kT} \frac{R(x)}{\mu_n} + \frac{q}{kT} \Psi' n' + \frac{q}{kT} n \frac{d\Psi'}{dx} \tag{4}$$

$$\frac{dp}{dx} = p' \tag{5}$$

$$\frac{dp'}{dx} = \frac{q}{kT} \frac{R(x)}{\mu_p} - \frac{q}{kT} \Psi' p' - \frac{q}{kT} p \frac{d\Psi'}{dx}, \tag{6}$$

and the boundary conditions,

$$\Psi(L) = 0 \tag{7}$$

$$n(L) = n_0 \tag{8}$$

$$p(L) = p_0 \tag{9}$$

$$\Psi'(0) = -\frac{\varepsilon_{ox}}{\varepsilon_s}\frac{V-\phi_{ms}-\Psi(0)}{\delta} - \frac{1}{\varepsilon_0\varepsilon_s}(Q_{ss}+Q_f) \tag{10}$$

$$\begin{aligned} n'(0) = {} & \frac{q}{kT}n(0)\,\Psi'(0) - \frac{q}{kT}\frac{n_0}{\mu_n}V_{cn} \\ & \times e^{-X_n^{1/2}\delta}\left(e^{-q(\delta V_{ox}-\Psi(0))/kT} - \frac{n(0)}{n_0}\right) \\ & + \frac{q}{kT}\frac{1}{\mu_n}\sum_i C_{ni}N_{ti}((1-f_i)\,n(0) - f_i n_{1i}) \end{aligned} \tag{11}$$

$$\begin{aligned} p'(0) = {} & \frac{q}{kT}p(0)\,\Psi'(0) - \frac{q}{kT}\frac{p_0}{\mu_p}V_{cp} \\ & \times e^{-X_p^{1/2}\delta}\left(e^{q(\delta V_{ox}-\Psi(0))/kT} - \frac{p(0)}{p_0}\right) \\ & + \frac{q}{kT}\frac{1}{\mu_p}\sum_i C_{pi}N_{ti}(f_i\,p(0) - (1-f_i)P_{1i}). \end{aligned} \tag{12}$$

The Runge–Kutta subroutine, used in the program, is based on Verner's fifth- and sixth-order pair of formulas for finding approximation to the solution of a system of equations. The integration step size is automatically chosen in order to keep the global error proportional to a tolerance specified by the user of the program and obtain the values of Ψ, n, p, Ψ', n', and p' at same time through every integration step.

The procedures of calculation for every applied voltage point are as follows:

(1) The trial values α_0, β_0, and γ_0 of the derivatives Ψ', n' and p' at $x = L$ are given by the boundary conditions (7)–(9).

(2) The values of Ψ, n, p, Ψ', n', and p' are calculated successively according to the Runge–Kutta method using Eq. (1)–(6) and the values of Ψ, n, p, Ψ', n', and p' at last point. At last, the prediction values of $\Psi(0)$, $n(0)$, $p(0)$, $\Psi'(0)$, $n'(0)$, and $p'(0)$ are obtained.

(3) The correction values, $\Psi_1'(0)$, $n_1'(0)$, and $p_1'(0)$, are obtained from the boundary conditions (10)–(12).

(4) The differences $F = \Delta\Psi'(0) = \Psi_1'(0) - \Psi'(0)$, $G = \Delta n'(0) = n_1'(0) - n'(0)$, and $H = \Delta p'(0) = p_1'(0) - p'(0)$ are dependent numerically on the trial value α, β, and γ at $x = L$. F, G, and H are the implicit functions of α, β, and γ. They can be expanded in first-order Taylor series:

$$F(\alpha,\beta,\gamma) = F_0(\alpha_0,\beta_0,\gamma_0) + \partial F/\partial x\,\Delta\alpha + \partial F/\partial\beta\,\Delta\beta + \partial F/\partial\gamma\,\Delta\gamma$$

$$G(\alpha,\beta,\gamma) = G_0(\alpha_0,\beta_0,\gamma_0) + \partial G/\partial\alpha\,\Delta\alpha + \partial G/\partial\beta\,\Delta\beta + \partial G/\partial\gamma\,\Delta\gamma$$

$$H(\alpha,\beta,\gamma) = H_0(\alpha_0,\beta_0,\gamma_0) + \partial H/\partial\alpha\,\Delta\alpha + \partial H/\partial\beta\,\Delta\beta + \partial H/\partial\gamma\,\Delta\gamma.$$

The partial derivatives $\partial F/\partial\alpha$, $\partial G/\partial\alpha$, $\partial H/\partial\alpha$, etc. are numerically calculated. Knowing that the solution corresponds to: $F(\alpha, \beta, \gamma) = G(\alpha, \beta, \gamma) = H(\alpha, \beta, \gamma) = 0$, the following three equations are established:

$$\begin{vmatrix} \frac{\partial F}{\partial\alpha} & \frac{\partial F}{\partial\beta} & \frac{\partial F}{\partial\gamma} \\ \frac{\partial G}{\partial\alpha} & \frac{\partial G}{\partial\beta} & \frac{\partial G}{\partial\gamma} \\ \frac{\partial H}{\partial\alpha} & \frac{\partial H}{\partial\beta} & \frac{\partial H}{\partial\gamma} \end{vmatrix} \begin{vmatrix} \Delta\alpha \\ \Delta\beta \\ \Delta\gamma \end{vmatrix} = - \begin{vmatrix} F_0 \\ G_0 \\ H_0 \end{vmatrix}.$$

Solving this set of equations, a new set of trial α_1 $(=\alpha_0+\Delta\alpha)$, β_1 $(=\beta_0+\Delta\beta)$, and γ_1 $(=\gamma_0+\Delta\gamma)$ are found.

(5) The above steps (2)–(4) are repeated until values of $\Delta F/F$, $\Delta G/G$, and $\Delta H/H$ are less than some limit, (i.e., 10^{-8}). The accuracy of results is significantly better than those resulting from the criteria $\Delta\Psi/\Psi < 10^{-5}$, $\Delta n/n < 10^{-4}$, and $\Delta p/p < 10^{-4}$, which are generally used in other numerical simulations.

The flowchart of the program is shown in Fig. 1. Our program, developed on HP1000 computer, has about 1500 FORTRAN statement lines and needs only memory 16K words. It can be easily transformed on minicomputer.

4. Results

We have used our program for a wide variety of situations: thickness of insulator varying from $\delta = 5$ Å (nearly metal-semiconductor contact) to $\delta = 50$ Å (thick tunnel diode); the thickness L of the substrate is taken less than the width of depletion layer W as in realistic actual VLSI applications. If $L > W$ (case of solar MIS tunnel diodes), the authors have shown that numerically simpler procedures can be used [12, 13]. In order to compare simulation results with experimental (I, V) characteristics TiW/Si Schottky diodes fabricated in Thomson Labs on $\langle 111 \rangle$ n-type Si($N_D = 1.5 \times 10^{16}$ cm^{-3}, $\phi_{ms} = 0.2$eV, $L = 0.4$ μm have been modeled (the device is an important element for STL logic circuit [15]).

The program allows, evidently, not only the simulation of I–V characteristics but also gives the evolution of internal physical parameters vs depth (density of injected carriers, distribution of potentials, Fermi levels, curents, electric field, carrier densities, etc.), so a very detailed physical analysis of examined structures can be obtained. The results of simulations are very close to experimental curves. In Figs. 2a and 2b typical examples of simulation are given.

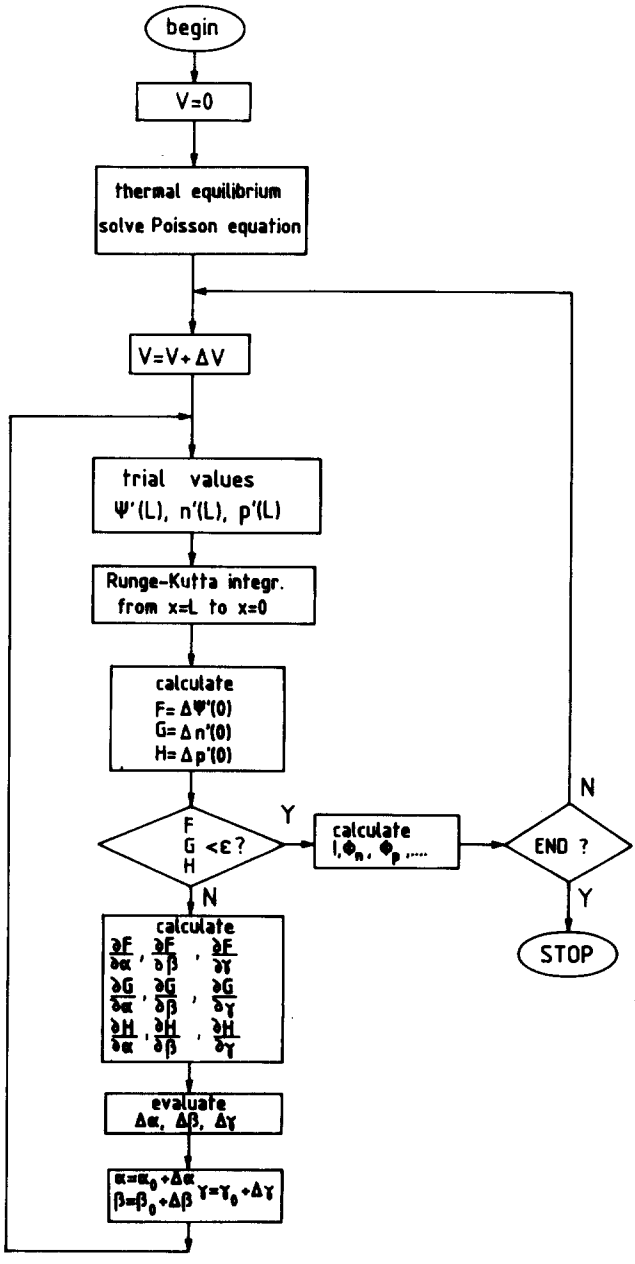

FIG. 1. The flowchart of the simulation program.

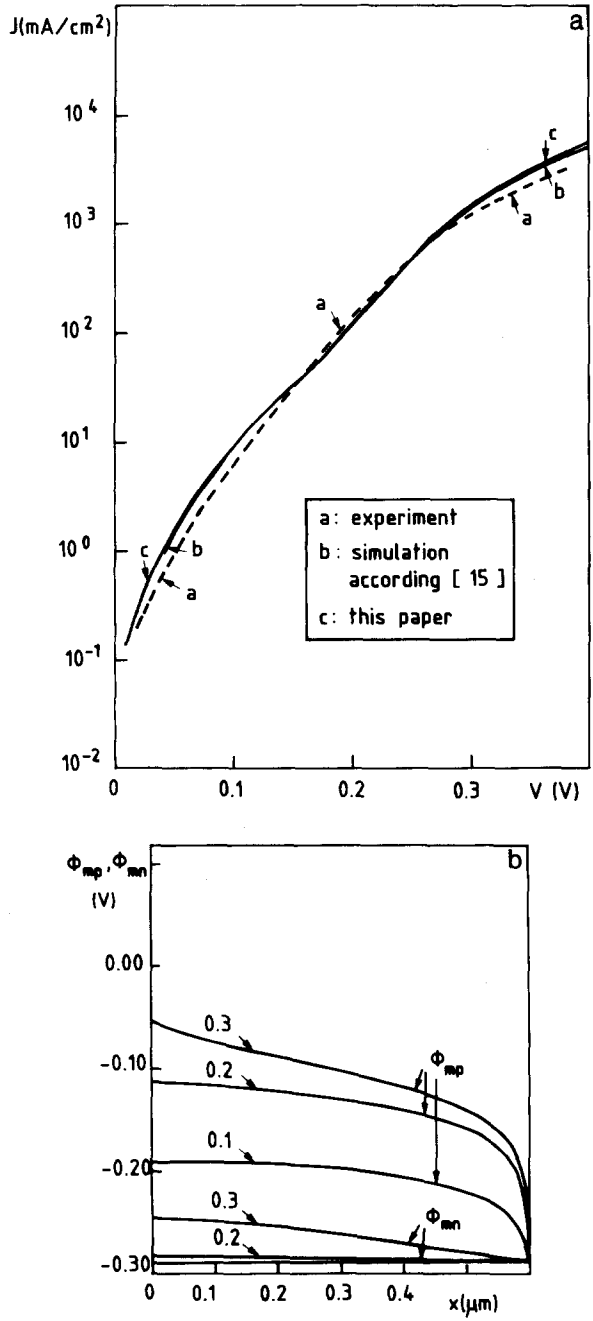

FIG. 2. (a) Experimental and theoretical (simulated) I–V characterization of a MIS Schottky diode with 0.5 nm thick oxide layer [15]. (b) Electron (ϕ_{mn}) and holes (ϕ_{mp}) quasi fermi levels vs x (forward bias).

5. Conclusion

The presented program allows a detailed analysis of realistic MIS tunnel structures. Specially it gives the possibility to characterize both kinetic and electristatic influences of interface states. It allows a rigorous study of the electrical behaviour of MIS devices and not only improves the understanding of their working but, also, indicates the technological modifications which should be operated to enhance STL circuits.

APPENDIX: List of Symbols

C_n, C_p: electron and hole capture coefficients
C_{ox}: oxide layer capacitance (per unit surface)
E: electric field
f: Schockley-Hall-Read interface states occupany
k: Boltzmann's constant
L: semiconductor layer thickness
N_D: semiconductor doping concentration
N_t: interface states density
n: semiconductor electron density; n_0 equilibrium value; $\Delta n = n - n_0$
p: semiconductor hole density; p_0 equilibrium value; $\Delta p = p - p_0$
q: electron charche
Q_{ss}: interface states charges (per unit area) at $x = 0$
Q_f: fixed charges (per unit area)
Q_{sc}: semiconductor space charge (per unit area)
Q_{mf}: oxide layer-metal contact frontal charge (per unit area) at $x = -\delta$
Q_{mb}: semiconductor-metal contact (back) charge (per unit area) at $x = L$
T: absolute temperature
V_{cn}, V_{cp}: electron and hole thermal velocities
V_{ox}: voltage drop accross the oxide layer; V_{oxo} equilibrium value; $\delta V_{ox} = V_{ox} - V_{oxo}$
R: Shockley–Hall–Read recombination rate
W: Space charge width
δ: oxide layer thickness
ε_0: vacuum permitivity
ε_{ox}, ε_s: oxide and semiconductor relative permitivity
μ_n, μ_p: electron and hole mobilities
ϕ_{ms}: metal-semiconductor work function difference
ψ: electrostatic potential.

References

1. S. Selberherr, *Analysis and Simulation of Semiconductor Devices* (Springer-Verlag, New York/Berlin, 1984).
2. M. Sanchez, *Electron Lett.* **3**, 117 (1967).

3. A. RALSTON AND H. S. WILF (Eds.), *Mathematical Method for Digital Computers*, Vol. 1 (Wiley, New York, 1960).
4. M. A. GREEN AND J. SHEWCHUN, *Solid-State Electron.* **17**, 349 (1974).
5. M. A. GREEN, F. D. KING, AND J. SHEWCHUN, *Solid-State Electron.* **17**, 551 (1974).
6. J. SHEWCHUN, M. A. GREEN, AND D. KING, *Solid-State Electron.* **17**, 563 (1974).
7. H. C. CARD, *Solid-State Electron.* **20**, 971 (1977).
8. E. D. ATHANASSOVA AND D. I. PUSKIKAROV, *Solid-State Electron.* **25**, 781 (1982).
9. N. G. TARR, L. PULFREY, AND D. S. CAMPORESE, *IEEE Trans. Electron Devices* **ED-30**, 1760 (1983).
10. C. Y. CHANG AND S. J. WANG, *Solid-State Electron.* **29**, 339 (1986).
11. P. CHATTOPADHYAY AND A. N. DAW, *Solid-State Electron.* **29**, 555 (1986).
12. G. PANANAKAKIS, G. KAMARINOS, AND P. VIKTOROVITCH, *Rev. Phys. Appl.* **14**, 639 (1979).
13. G. PANANAKAKIS AND G. KAMARINOS, *NASECODE* **3**, 225 (1983).
14. S. M. SZE, *Physics of Semiconductors Devices* (Wiley International, New York, 1969).
15. G. PANANAKAKIS, B. ANDRIES, G. KAMARINOS, AND T. BARSOTTI, *ESSDERC'86, Cambridge (UK), European Physical Society*, 10*G*, Sept. 1986, p. 168.

RECEIVED: January 5, 1989; REVISED: October 4, 1989

YONGWEI XIA
GEORGES PANANAKAKIS
GEORGES KAMARINOS

Laboratoire de Physique des Composants à Semiconducteurs
C.N.R.S. UA 840-ENSERG, B.P. 257
38016-Grenoble Cedex, France